J. Min. Metall. Sect. B-Metall. 48 (1) B (2012) 73 - 79

Journal of
Mining and
Metallurgy

SOLIDIFICATION CHARACTERISTICS OF ATOMIZED AlCu4Mg1-SiC COMPOSITE POWDERS

R. Yamanoglu[#,*], M. Zeren[*], Randall M. German[**]

Department of Metallurgical and Materials Engineering, Kocaeli University,
Umuttepe Campus, Kocaeli 41380, Turkey
Department of Mechanical Engineering, San Diego State University,
San Diego, California 92182-1323, USA

(Received 17 July 2011; accepted 26 August 2011)

Abstract

In this study, rapidly solidified metal matrix composite powders have been produced by PREP (Plasma rotating electrode process) atomization. AlCu4Mg1 alloy is used as the matrix material while SiC particles, with about 650 nm average particle size, are used as the reinforcement phase. The microstructural and solidification characteristics of composite particles are studied using optical and scanning electron microscope (SEM). The relationship between secondary dendrite arm spacing (SDAS) and particle diameter was examined, and these composite powders were found to have dendritic and equiaxed solidification with a fine eutectic phase. SDAS measurements using various sized particles show that secondary dendrite arm spacing slightly decreases with the decrease in particle size.

Keywords: Al-SiC powders, composite, powder metallurgy, rapid solidification.

1. Introduction

SiC/Al composites are preferred for many applications due to their high specific modulus, strength, and thermal stability. Because of these properties, SiC/Al composites are used in the aerospace and automobile industries, in applications such as electronic heat sinks, drive shafts, ground vehicle brake rotors, jet fighter aircraft fins, or engine components [1-3].

Aluminum and its alloys are remarkable for structural applications due to the requirements of lighter and stronger

[#] *Corresponding author: ryamanoglu@gmail.com*

DOI:10.2298/JMMB110717005Y

materials [4-5]. Powder metallurgy and mechanical alloying are sophisticated technologies for structural hardening of Al-based alloys. A hardening effect is obtained for Al-based materials with very fine metal oxides and carbides [6]. The nature of the interface between the matrix and the additional material has an important role in defining the characteristics of the composite, particularly the physical and chemical coherence between the SiC particles and aluminum matrix in the preparation of SiC/Al composites [7-8].

Rapidly solidified particles exhibit a number of advantages, including a smaller scale of the microstructure than conventional routes [9]. Rapid solidificaton properties are described by measuring secondary dendrite arm spacing (SDAS), which is the most important metallurgical factor that affects the mechanical properties of the materials [10]. A decrease in the SDAS value increases the ultimate tensile strength and elongation. SDAS is controlled by the solidification time [11].

In the present study, rapidly solidifed composite powders were fabricated by plasma rotating electrode process (PREP) atomization. PREP is a useful technique to produce rapidly solidified spherical powders with low impurity levels [12]. The effect of rapid solidification on the microstructure was investigated in detail.

2. Experimental

Al-Cu-Mg alloy was used as the matrix material in this study. The chemical composition of the matrix material is $_{0.42}$Si-$_{0.52}$Fe-$_{4.01}$Cu-$_{0.43}$Mn-$_{1.36}$Mg-$_{0.13}$Cr-$_{0.03}$Zn-$_{0.01}$Ti-$_{remainder}$Al(wt-%). Prior to atomization, SiC particles with an average diameter of 650 nm were added during casting of the alloy. The composition was mechanically mixed to provide homogeneous distribution of the reinforced particles. After casting, the composite material was extruded to get an anode bar with 55 mm diameter. In order to manufacture the rapidly solidified Al-SiC composite powder, the anode bar was atomized by PREP under Ar atmosphere with a pressure of 1.3 atm. In this process, the surface of a rotating electrode bar is melted by using a high-temperature plasma arc within a controlled atmosphere chamber of 2.5 m in diameter. The molten droplets are ejected from the surface of the bar by centrifugal forces. A schematic sketch is shown in Figure 1.

The rotation speed of the 55 mm diameter anode bars were 3500, 8000 and 12000 rev/min, to produce powders with different particle size distribution. The evolution of the microstructure of the anode bar and produced particles were investigated by microscopy. All specimens were polished and etched with Keller's reagent, with an etching time of 20 seconds. The microstructure images were obtained using an optical microscope (Zeiss Axiophot) and a Scanning Electron Microscope (JEOL 6060).

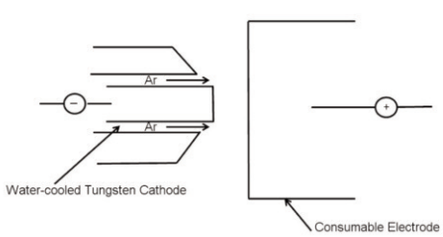

Figure 1. Schematic of PREP set-up

A Quantimet 501 Image analyzer was used to measure the secondary dendrite arm spacing of different sized particles.

3. Result and Discussion

An optical micrograph of the hot extruded Al-Cu4-Mg1 alloy particulated with SiC particles (the anode bar) is shown in Figure 2. The microstructure of the extruded bar shows a coarse dendritic pattern with SiC particles distributed mainly in the interdendritic area (as seen in Figure 2b). Average secondary dendrite arm spacing of this extruded bar was measured as 54 μm, due to the low cooling rate.

After atomization of the composite powders, as-solidified particles were sieved depending on rotation speed. Median particle sizes of each rotation speed (3500, 8000 and 12000 rev/min) are 550 μm, 240 μm, and 170 μm respectively. Increased rotational speed produced smaller median sized particles. Scanning electron micrographs of the powders produced by PREP reveal a mostly spherical shape. The morphology of the particles is shown in Figure 3. The particles were spheroidised due to surface tension and the droplets minimise their surface energy by forming a sphere. The size and shape of the particles depends on solidification and spheroidization time. Calculated solidification and spheroidisation parameters are shown in Table 1 [13]. It is clear that spheroidisation time is significantly shorter than the solidification time, giving the observed spheres.

The solidified particles showed microstructures consisting of dendritic and equiaxed structures embedded in a fine eutectic phase. Scanning electron

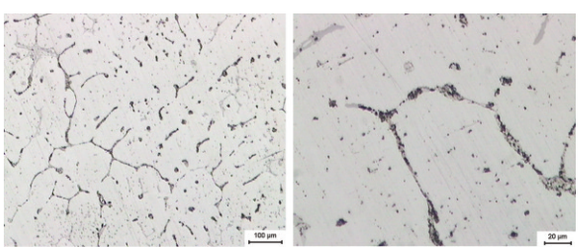

Figure 2. Optical micrographs of extruded alloy, a) low, b) high magnification

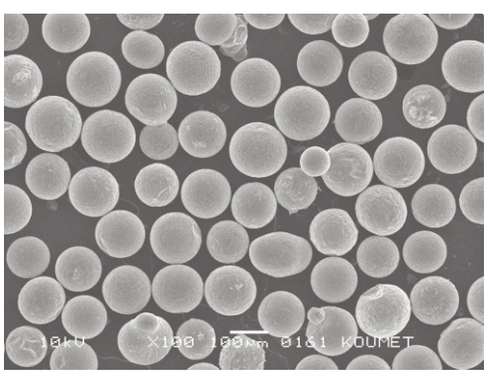

Figure 3. SEM image of PREPed Al-SiC powders

Table 1. The solidification and spheroidization parameters of Al-SiC composite powders

Rotation speed (rpm)	electrode diameter (mm)	measured median size (μm)	predicted median size (μm)	solidification time (ms)	spheroidization time (μs)	particle shape
3500	55	550	584	140	1,1	Sphere
8000	55	240	256	63	0,35	Sphere
12000	55	170	170	42	0,15	Sphere

microscopy observations were performed to investigate these formation of the particles. Figures 4a and 4b show that the microstructure of the particles consists of dendritic and equiaxed structures, respectively. Figure 5 also shows primary dendritic solidification, with a fine eutectic in the interdendritic regions.

The eutectic structure is best recognized using optical microscopy, as shown in Figure 6. A fine eutectic area (dark region) can be seen between primary coarse Al-rich dendrites (light area).

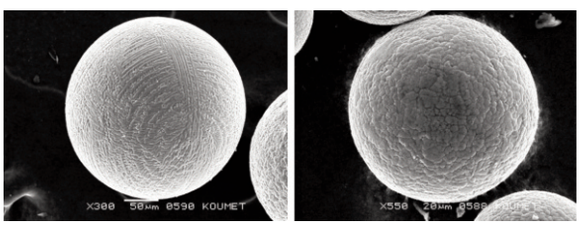

Figure 4. SEM images of particles, a) dendritic, b) equiaxed structure

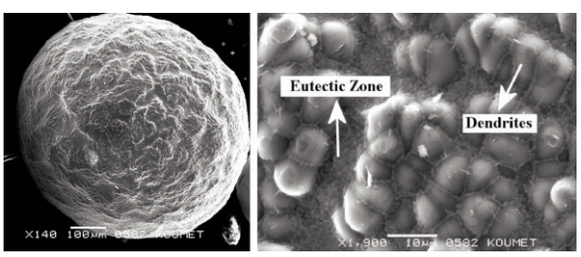

Figure 5. Dendritic solidification with a fine eutectic, a) low, b) high magnification

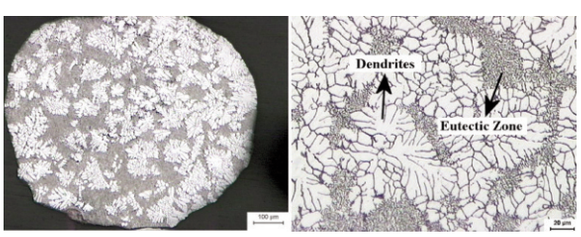

Figure 6. Eutectic phase between primary aluminum dendrites, a) low, b) high magnification

Al-rich dendrites are due to the high cooling rate of the solidification of the micron-sized droplets, creating a small interlamellar spacing. A more detailed image of the eutectic phase is shown in Figure 7.

Since the dendrite arm spacing is directly related to the rate of solidification, secondary dendrite arm spacings (SDAS) are measured to determine the effect of solidification conditions on the microstructure of Al–Cu–Mg alloys. Cooling rate is an important factor on the solidification of powders. Primary solidification occurs in the dendritic form. If the cooling rate increases, particle size decreases, and a higher cooling rate causes finer and more homogeneous dendrites [14]. Secondary dendrite arm spacing (SDAS) was measured to describe the relation between particle size and cooling rate. Different-sized powders were selected to determine the dendrite arm spacing (Table 2).

These values indicate that SDAS depends on particle size and cooling rate. Smaller particles which have high cooling rate have smaller SDAS. The relationship between particle size and SDAS for Al-SiC powders is compared the data by Gahm, et al., shown in Figure 8 [15] and by Zeren in Figure 9 [14]. Figure 8 shows that SDAS decreases with smaller particles due to high cooling rate in the PREP process compared with

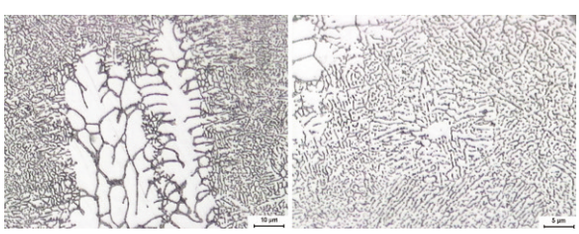

Figure 7. Fine eutectic phase in a composite particle, a) low, b) high magnification

other studied materials. The finer particles are expected to undercool more and thus yield finer secondary dendrite arm spacing. Cooling rate can be estimated according to Figure 9. PREPed Al-SiC powders have different cooling rates, ranging from 10^1 and 10^5 K/s, which create different particle sizes.

The relationship between SDAS and other production methods is shown in Table 3. PREPed powders showed significantly smaller secondary dendrite arm spacing due to high cooling rate, compared to different conventional casting techniques.

The composite particles also showed an

Table 2. SDAS results for different-sized powders.

SDAS		
Powder Diameter (μm)	Average Distance (μm)	SD (standard deviation)
47	0,85	0,17
250	4,16	1,29
450	9,97	2,50

Table 3. SDAS of different aluminum alloys.

Different studies	SDAS (μm)
Present work (as atomized)	0,85-9,97
Present work (as casted and extruded)	54
Guo-fa at al.(chill casted) (16)	20 – 120
Lim, C.S at al. (investment casted) (11)	33,31
Lim, C.S at al. (pressure assisted investment casted) (11)	74
Lim, C.S at al. (11) (squeeze casted)	11,43
Lopez at al. (17) (as casted)	23-104

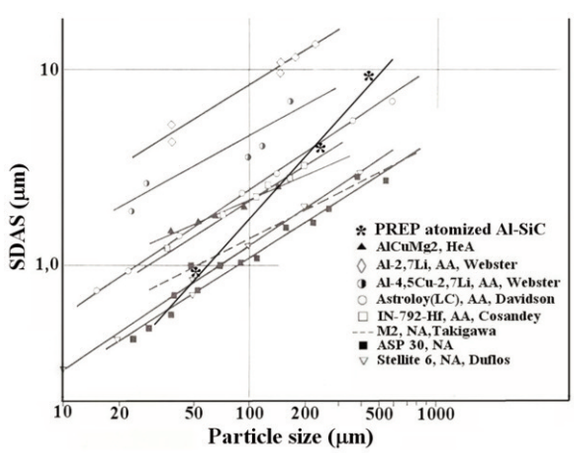

Figure 8. Secondary dendrite arm spacings versus particle size (15)

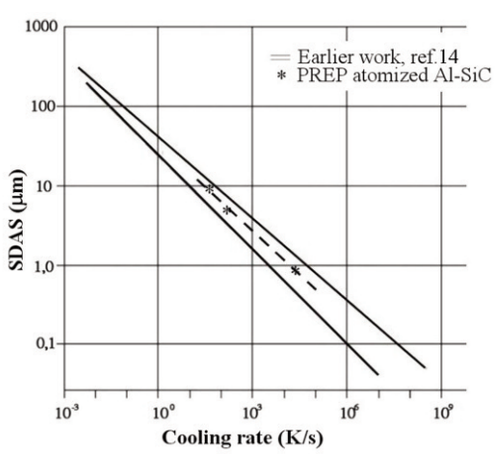

Figure 9. Secondary dendrite arm spacings versus cooling rate

eutectic melting during atomization (Figure 10). The alloy contains localized regions of Al_2Cu and Mg_2Si eutectic phases as provided by X-ray diffraction pattern presented in Figure 10. These high solute regions melt at temperatures below the equilibrium solidus. If this alloy is brought to high temperature too rapidly, it can present localized eutectic melting as shown in Figure 11 [18].

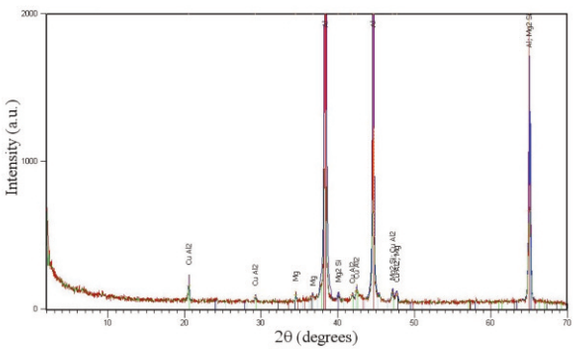

Figure 10. XRD patterns of as atomized Al-SiC powders

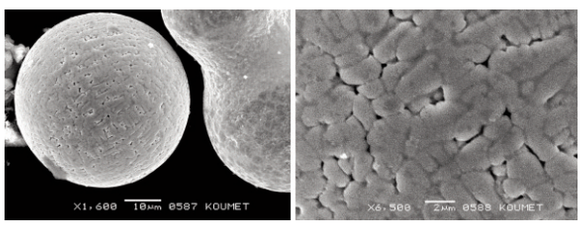

Figure 11. Local eutectic melting on the PREPed particles, a) low, b) high magnification

4. Conclusion

The aluminum alloy reinforced with SiC particles was succesfully produced by powder metallurgical plasma rotating electrode (PREP) process. The solidification properties of PREPed particles and wrought material have been compared. The increase of rotation speed of the anode bar in PREP atomization provides an effective reduction of the particle size. The solidified Al-composite powders showed microstructure consisting of dendritic and equiaxed structures in a fine eutectic phase. Secondary dendrite arm spacing is slightly decreased in smaller particles, depending on cooling rate. The dendrite size is reduced as a result of rapid solidification, compared to the conventionally cast and extruded alloys. Some particles showed eutectic melting due to high temperature during plasma melting.

Acknowledgement

The authors special thank the Scientific Research Projects Unit of Kocaeli University.

References

[1] H. Wang, R. Zhang, X. Hu, C. Wang, Y. Huang, J. Mater. Process. Technol., 197 (2008) 43.

[2] R. Anandkumar, A. Almeida, R. Colaço, R. Vilar, V. Ocelik, J. Th M. De Hosson, Surf. Coat. Technol., 201 (2007) 9497.

[3] M. Song, T. Nonferr. Metal. Soc., 19 (2009) 1400.

[4] H. R. Zaid, A. M. Hatab, A. M. A. Inrahim, J. Min. Metall. Sect. B., 47 (1) (2011) 31.

[5] N. Dolic, J. Malina, A. Begic Hadzipasic, J. Min. Metall. Sect. B., 47 (1) (2011) 79.

[6] L. Blaz, M. Sugamata, G. Wloch, J. Sobota, A. Kula, J. Alloys. Compd., 506 (2010) 179.

[7] R. M. Wang, M. K. Surappa, C. H. Tao, C. Z. Li, M. G. Yan, Mat. Sci. Eng. A-Struct., 254, (1998) 219.

[8] B Xiong, Z. Xu, Q. Yan, B. Lu, C. Cai, J. Alloys. Compd., 509 (2011) 1187.

[9] K. T. Conlon, E. Maire, D. S. Wilkinson, H. Henein, Metall. Mater. Trans. A., 31 (2000) 249.

[10] Z. Chen, Y. Lei, H. Zhang, J. Alloys. Compd., 509 (2011) 7473.

[11] C. S. Lim, A. J. Clegg, N. L. Loh, J. Mater. Process. Tech., 70 (1997) 99.

[12] S. Hata, T. Hashimoto, N. Kuwano, K. Oki, J. Phase Equilib., 22 (2001) 386.

[13] R. M. German, Powder Metallurgy & Particulate Materials Processing, Princeton, NJ, MPIF, (2005) 84.

[14] M. Zeren, J. Mater. Process. Tech., 169 (2005) 292.

[15] H. Gahm, K. D. Löcker, H. Fischmeister, S. Karagöz, A. Gruber, F. Jeglitsch, Pract. Metallogr., 18 (1987) 479.

[16] M. Gu-fa, L. Xiang-yu, Z. Zhao-jun, W. Hong-wei, T. Nonferr. Metal. Soc., 17 (2007) 1012.

[17] C. Vazquez-lopez, A. Calderon, M. E. Rodriguez, E. Velasco, S. Cano, R. Colas, S. Valtierra, J. Mater. Res., 15 (2000) 85.

[18] D. J. Chakrabarti, J. L. Murray, Mater. Sci. Forum, 217 (1996) 177.